DNA-based thermoelectric devices: A theoretical prospective

Enrique Maciá
Departamento de Física de Materiales, Facultad CC. Físicas, Universidad Complutense de Madrid, E-28040, Madrid, Spain
(Received 17 August 2006; revised manuscript received 20 October 2006; published 30 January 2007)

The thermoelectric performance of PolyG-PolyC and PolyA-PolyT double-stranded chains connected between organic contacts at different temperatures is theoretically studied on the basis of an effective model Hamiltonian. The obtained analytical expressions reveal the existence of important resonance effects leading to a significant enhancement of the Seebeck coefficient depending on the Fermi level position. High thermoelectric power factors, up to $P=(1.5-3)\times 10^{-3}$ W m^{-1} K^{-2}, are obtained close to the resonance energy. These values suggest that significantly high values of the thermoelectric figure of merit may be attained for synthetic DNA samples at room temperature. The possibility of combining *p*-type and *n*-type synthetic DNA chains in the design of a nanoscale Peltier cell is discussed, taking into account both contact and environmental effects.

DOI: 10.1103/PhysRevB.75.035130 PACS number(s): 87.14.Gg, 71.20.−b, 72.10.−d, 72.80.Le

I. INTRODUCTION

The experimental way to the possible use of organic molecules in the design of nanoscale thermoelectric devices was opened up by the measurement of an appreciable thermoelectric power (+18 μV K^{-1} at room temperature) over guanine molecules adsorbed on a graphite substrate using a scanning tunneling microscope tip.[1] Subsequently, the thermoelectric response of phenyldithiol organic molecules chemisorbed on gold surfaces was theoretically analyzed, and Seebeck coefficient values comparable to those obtained in Poler's experiment were reported.[2] Similar values (+22 μV K^{-1} at room temperature) have been recently reported on a sample of $FeCl_3$-doped polythiophene.[3] Although these figures are too small to be of interest for most current thermoelectric applications, it is reasonable to expect that they may be significantly enhanced by a proper choice of the materials composing the thermoelectric nanocell. Thus, the thermoelectric potential of some conducting polymers, like polythiophene and polyaminosquarine, has been recently reviewed on the basis of their electronic band structures.[3] Also, the thermoelectric properties of nanocontacts made of single-wall carbon nanotubes have been studied numerically, concluding that doped semiconducting nanotubes may exhibit very high figures of thermoelectric merit.[4] In fact, the extreme sensitivity of thermopower to finer details in the electronic structure suggests that one could optimize the device's thermoelectric performance by properly engineering its electronic structure. With the aim of exploring such a possibility, we performed a systematic theoretical study on the thermoelectric properties of DNA nucleobases guanine (G), cytosine (C), adenine (A), and thymine (T)—either as single units or forming dimers or trimers—connected to metallic leads at different temperatures.[5–7] The results showed that relatively large thermopower values can indeed be obtained by properly locating the system's Fermi level.[6,7] In addition, the thermoelectric response of trimer nucleobases exhibits two resonant features where the Seebeck coefficient attains large values (200–400 μV K^{-1} at room temperature), closely resembling recently reported thermopower curves of silicon-based atomic junctions.[8] Since both the location and the magnitude of these peaks sensitively depend on the energetics of the considered trimer, one may think of introducing a thermoelectric signature for different codons of biological interest,[7] in close analogy with the transversal electronic signature recently proposed for single-stranded DNA chains.[9,10]

In this work, we will analyze the thermoelectric response of more realistic double-stranded DNA (dsDNA) chains, hence extending our previous results in order to perform a theoretical prospective on the potential of synthetic DNA chains as thermoelectric materials. Duplex DNA molecules can be classified into biological (i.e., samples extracted from living organisms) and artificially engineered molecules [e.g., poly(dG)-poly(dC) or poly(dA)-poly(dT) chains]. Synthetic nucleic acids considered so far are oligonucleotides where relatively few base pairs (BPs) are periodically arranged. These molecules are quite different from the biological ones, in which thousands to millions of BPs, including four different nucleotides, are aperiodically distributed.[11] Nevertheless, the nature of charge transport in both kinds of DNA chains can be traced back to a common mechanism, based on the aromatic base stacking between adjacent nucleotides, which promotes charge delocalization over a certain length.[12] From an applied viewpoint the convenience of synthetic versus biological DNA based thermoelectric devices is twofold: (i) synthetic DNA strands can be polymerized at will in order to fit any prescribed design; and (ii) quantum chemical calculations show the existence of convenient charge channels in periodic dsDNA chains. Thus, charge transfer mainly proceeds via hole (electron) propagation through the purine (pyrimidine) bases, where the highest occupied (HOMO) [lowest unoccupied (LUMO)] molecular orbital carriers are respectively located in polyG-polyC (polyA-polyT) chains.[13,14] In fact, experimental current-voltage curves show that double-stranded poly(dA)-poly(dT) chains behave as *n*-type semiconductors, whereas poly(dG)-poly(dC) ones behave as *p*-type semiconductors.[15] Accordingly, these synthetic DNAs may provide the basic building blocks necessary to construct a nanoscale thermoelectric cell, where the DNA chains will play the role of semiconducting legs in standard Peltier cells, as illustrated in Fig. 1.

In order to further substantiate this proposal, in this work we present a theoretical study on the energy dependence of Seebeck coefficient S and thermoelectric power factor ($S^2\sigma$, where σ is the electrical conductivity) of polyG-polyC and

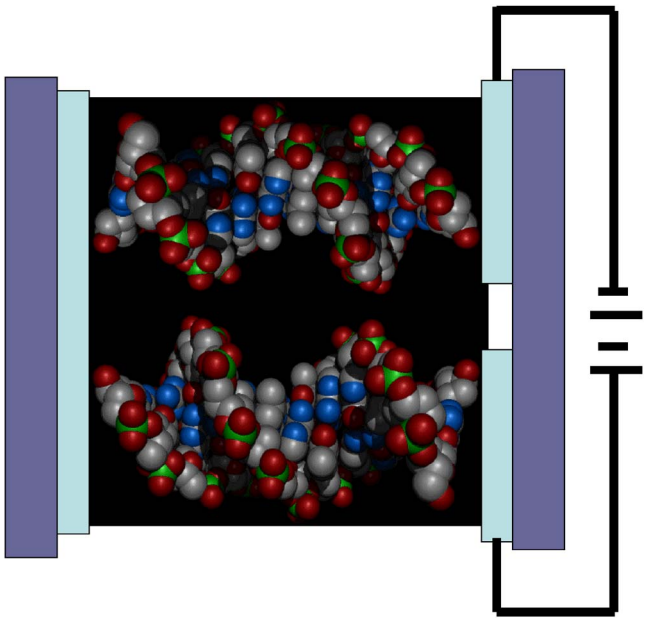

FIG. 1. (Color online) Sketch illustrating the basic features of a nanoscale DNA-based Peltier cell. A polyA-polyT (polyG-polyC) oligonucleotide, playing the role of *n*-type, left (*p*-type, right) semiconductor legs, is connected to organic wires (light boxes) deposited onto ceramic heat sinks (dark boxes).

polyA-polyT chains at room temperature. Following our previous work, we model the duplex DNA molecules in terms of a renormalized one-dimensional effective Hamiltonian whose transmission coefficient at zero bias is analytically derived by embedding the chain between two semi-infinite leads.[16] From the knowledge of the transmission spectrum the thermoelectric voltage is then obtained making use of the approach introduced by Paulsson and Datta.[2] In this way, we derive closed analytical expressions describing the Seebeck coefficient and power factor dependences on the Fermi level position for synthetic DNA chains. According to the obtained results, polyG-polyC and polyA-polyT oligomers appear as promising thermoelectric materials to be used in the design of DNA-based, nanoscale thermoelectric devices.

II. MODEL DESCRIPTION

Transport experiments have shown that chemical bonding between DNA and metal electrodes is a prerequisite for achieving reproducible conductivity results.[17–24] Thus, the binding of DNA to the metallic leads could affect the electronic structure of the molecule itself.[25,26] Fortunately, in the DNA-metal junction case, one can restrict the analysis to the weak coupling limit,[12,27] and consider the following one-dimensional effective Hamiltonian,[16]

$$\sum_{n=1}^{N} [\alpha(E)c_n^{\dagger}c_n - t_0 c_n^{\dagger}c_{n+1} + \text{H.c.}] - \tau(c_0^{\dagger}c_1 + c_{N+1}^{\dagger}c_N + \text{H.c.}) + \sum_{n=0}^{-\infty} (\varepsilon_M c_n^{\dagger}c_n - t_M c_n^{\dagger}c_{n+1} + \text{H.c.}) + \sum_{n=N+1}^{+\infty} (\varepsilon_M c_n^{\dagger}c_n - t_M c_n^{\dagger}c_{n+1} + \text{H.c.}), \quad (1)$$

where $c_n^{\dagger}$ (c_n) is the creation (annihilation) operator for a charge at the nth site in the chain and N is the number of BPs. The first term describes the charge carrier propagation through the original dsDNA chain in terms of an equivalent monatomic lattice, where the renormalized "atoms" α correspond to the Watson-Crick complementary pairs in the original DNA molecule, and t_0 is the hopping integral describing the aromatic base stacking between adjacent nucleotides. The renormalized on-site energies enclose the quantum description of the Watson-Crick BP energetics through the expression[16]

$$\alpha(E) = b + a_1 E + \frac{2t^2}{E-\gamma}, \quad (2)$$

where (depending on the considered DNA molecule) $b \equiv a_0 - \gamma a_1$, $a_0 \equiv t_{GC(AT)} + 2(\varepsilon_{G(A)} + \varepsilon_{C(T)})$, $a_1 \equiv (\varepsilon_{G(A)}^2 + \varepsilon_{C(T)}^2)/t^2$, $t_{GC(AT)}$ describes the hydrogen bonding between the complementary bases, ε_k are the nucleobase on-site energies, t describes the hopping integral between a backbone state and the base state,[28] and γ accounts for the sugar-phosphate backbone on-site energies. Note that the renormalized DNA lattice includes six physical parameters $\{\varepsilon_{G(A)}, \varepsilon_{C(T)}, t_{GC(AT)}, t, \gamma, t_0\}$ fully describing the most relevant physics of the DNA molecule in terms of just two basic variables (α, t_0). The second term in Eq. (1) describes the DNA-lead contacts, where τ measures the coupling strength between the leads and the end nucleotides. Modeling the geometry and bonding character of the contact at the interface is a very delicate issue, since detailed information on the metal geometry and DNA chemical bonding at the contacts is poorly known to date. Consequently, in our modeling of the DNA contact, the parameter τ deals with the tunneling probability between the frontier orbitals, roughly describing bonding effects at the interface. Finally, the last two terms describe the leads at both sides of the DNA chain, modeled as semi-infinite one-dimensional chains of atoms with one orbital per site, where ε_M is the on-site energy and t_M is the hopping term.

III. ANALYTICAL EXPRESSIONS

Within the transfer matrix framework, considering nearest-neighbor interactions only, the Schrödinger equation corresponding to the Hamiltonian (1) can be expressed in the form

$$\begin{pmatrix} \psi_{N+1} \\ \psi_N \end{pmatrix} = \begin{pmatrix} 2x\lambda^{-1} & -\lambda^{-1} \\ 1 & 0 \end{pmatrix} \begin{pmatrix} 2x & -1 \\ 1 & 0 \end{pmatrix}^{N-2} \begin{pmatrix} 2x & -\lambda \\ 1 & 0 \end{pmatrix} \begin{pmatrix} \psi_1 \\ \psi_0 \end{pmatrix}, \quad (3)$$

where ψ_n is the wave function amplitude for the energy E at site n, $2x \equiv (E-\alpha)/t_0$ describes the DNA energetics, and the ratio $\lambda \equiv \tau/t_0$ measures the DNA-lead coupling strength. The transmission coefficient at zero bias as a function of energy is given by[16]

$$T_N(E) = \{1 + W^{-1}[(E - \varepsilon_M)U_{N-1} - \Omega(U_N + \lambda^2 U_{N-2})]^2\}^{-1}, \tag{4}$$

where $W \equiv (E-E_-)(E_+-E)$, with $E_\pm \equiv \varepsilon_M \pm 2t_M$, define the allowed spectral window determined by the lead bandwidth, $\Omega \equiv t_M/\lambda$, and $U_k(x) \equiv \sin[(k+1)\theta]/\sin\theta$, with $x \equiv \cos\theta$, are Chebyshev polynomials of the second kind. By inspecting Eq. (4) we realize that the transmission coefficient in general does not reach the full transmission condition $T_N=1$. This transmission degradation stems from contact effects.[27] In fact, even in the most favorable conditions for charge transport (i.e., $E=\varepsilon_M$) we get $T_N(\varepsilon_M)=[1+(\lambda U^*_{N-2} + \lambda^{-1}U^*_N)^2/4]^{-1} < 1$, where $U^*_k \equiv U_k(x_M)$, and $2x_M=[\varepsilon_M - \alpha(\varepsilon_M)]/t_0$.

From the knowledge of the transmission coefficient given by Eq. (4) the conductance through the lead-DNA-lead system is determined using the Landauer formula[29]

$$G_N(E_F) = G_0 T_N(E_F), \tag{5}$$

where $G_0=2e^2/h \simeq 1/12\,906\ \Omega^{-1}$, and E_F denotes the Fermi level. On the other hand, the Seebeck coefficient is obtained from the expression[2]

$$S_N(E_F,T) = -|e|L_0\left(\frac{\partial \ln T_N(E)}{\partial E}\right)_{E_F} T, \tag{6}$$

where e is the electron charge, $L_0 \equiv \pi^2 k_B^2/3e^2 = 2.44 \times 10^{-8}\ \mathrm{V^2\,K^{-2}}$ is the Lorenz number, and T is the temperature. Making use of Eqs. (4) and (5) in Eq. (6) one gets

$$S_N(E_F,T) = \widetilde{S}_0(T)\Delta G \left\{ B(E_F) + \left(\frac{\partial \ln[(E-\varepsilon_M)U_{N-1} - \Omega(U_N + \lambda^2 U_{N-2})]}{\partial E}\right)_{E_F} \right\}, \tag{7}$$

where $\widetilde{S}_0(T) = 2|e|L_0 T$, $\Delta G \equiv 1 - G_N/G_0$, and $B(E_F) \equiv (E_F - \varepsilon_M)/W(E_F)$. The Seebeck coefficient is then expressed as a product involving three contributions. The factor $\widetilde{S}_0$ sets the thermovoltage scale (in $\mu\mathrm{V\,K^{-1}\,eV}$ units) and accounts for the linear temperature dependence of S_N.[30] The factor ΔG links the thermopower magnitude to the conductance properties of the chain, so that the Seebeck coefficient progressively decreases (increases) as the conductance increases (decreases), vanishing when $T_N=1$, as expected from basic transport theory. The last factor in Eq. (7) depends on two additive contributions in turn. The value of $B(E_F)$ depends on the relative position of the Fermi level with respect to both the center, ε_M, and the band edges, $E_\pm$, of the contacts. Thus, its contribution vanishes when $E_F \to \varepsilon_M$, whereas B (and consequently S_N) asymptotically diverges as the Fermi level approaches the spectral window edges (i.e., $E_F \to E_\pm$). Finally, the logarithmic derivative term in Eq. (7) contains most physically relevant information, accounting for (i) contact effects (related to the coupling constants λ and Ω), (ii) size effects (described by the N parameter dependence), and (iii) resonance effects related to the DNA energetics by means of the Chebyshev polynomials' argument

$$x(E_F) \equiv x_0 = -\frac{1}{2t_0}\left(b + AE_F + \frac{2t^2}{E_F - \gamma}\right), \tag{8}$$

where $A \equiv a_1 - 1$. In this work we are mainly interested in the study of the *intrinsic* transport properties of DNA chains, so that we will minimize contact effects by adopting $t_M = t_0 = \tau$ henceforth, so that $\lambda=1$ and $\Omega=t_0$.[31] Thus, taking into account the recurrence relationship $U_{k+1} - 2xU_k + U_{k-1} = 0$, we can rewrite Eqs. (5) and (7) in the form

$$G_N(E_F) = \frac{G_0}{1 + C(E_F)U^2_{N-1}}, \tag{9}$$

where $C(E_F) \equiv [\alpha(E_F) - \varepsilon_M]^2/W(E_F)$, and

$$S_N(E_F,T) = \widetilde{S}_0(T)[1 - T_N(E_F)] \times \left[B(E_F) + \frac{P_2(E_F)}{E_F - \gamma} + \left(\frac{\partial \ln U_{N-1}}{\partial E}\right)_{E_F}\right], \tag{10}$$

where

$$P_2(E_F) \equiv \frac{a_1(E_F-\gamma)^2 - 2t^2}{a_1(E_F-\gamma)^2 + (a_0 - \varepsilon_M)(E_F - \gamma) + 2t^2}. \tag{11}$$

By comparing Eqs. (7) and (10) we see that the logarithmic derivative in Eq. (7) has been split into two separate contributions. The first one includes sugar-phosphate backbone effects through the γ parameter dependence. In particular, since $P_2(\gamma) = -1$, we realize that S_N asymptotically diverges as the Fermi level approaches the backbone on-site energy (i.e., $E_F \to \gamma$). In general, the γ value will depend on the chemical nature of the nucleotides, as well as the possible presence of water molecules and/or counterions attached to the backbone.[12,16] Accordingly, this resonant enhancement of thermoelectric power strongly depends on environmental conditions affecting the DNA electronic structure. Finally, the Chebyshev polynomial logarithmic derivative appearing in Eq. (10) describes possible size effects in the thermoelectric response for DNA chains of different length.

Making use of the mathematical relation

$$\frac{dU_{k-1}}{dx} = \frac{xU_{k-1} - k\widetilde{T}_k}{1 - x^2}, \tag{12}$$

where $\widetilde{T}_k(x) \equiv \cos(k\theta)$ is a Chebyshev polynomial of the first kind, we express Eq. (10) in the explicit form

$$S_N(E_F,T) = \frac{\widetilde{S}_0(T)}{1 + C^{-1}U^2_{N-1}(x_0)} \times \left[F(E_F) + \frac{D(E_F)}{1 - x_0^2}\left(N\frac{\widetilde{T}_N(x_0)}{U_{N-1}(x_0)} - x_0\right)\right], \tag{13}$$

which is more convenient for numerical purposes, where $F(E_F) \equiv B(E_F) + P_2(E_F - \gamma)^{-1}$, $2D(E_F) \equiv [A - 2t^2(E_F - \gamma)^{-2}]t_0^{-1}$, and we have explicitly assumed $U_{N-1} \neq 0$ and $C \neq 0$ (otherwise we get the trivial case $S_N=0$).

TABLE I. Parameters adopted for the effective Hamiltonian considered in this work arranged by decreasing energies.

Model Hamiltonian parameters (eV)	
$\gamma=12.27$	
$\varepsilon_A=8.25$	$\varepsilon_T=9.13$
$\varepsilon_G=7.77$	$\varepsilon_C=8.87$
$t=1.5$	
$t_{GC}=0.90$	$t_{AT}=0.34$
$t_0=0.15$	

IV. DISCUSSION

A. Model parameter values

We will evaluate the electric conductance and thermopower curves given by Eqs. (9) and (13) at room temperature making use of the model parameters listed in Table I. The on-site energies for the different nucleobases are chosen as the ionic potentials of their *N*-methylated forms.[32] On the basis of a recent study about Hückel parameters for biomolecules we adopt the value $\gamma=4.5$ eV for the backbone phosphate group on-site energy and the value $t=1.5$ eV for the resonance integral between the nucleobases and the sugar moiety.[28] The precise nature of hydrogen bonding in a Watson-Crick BP has been the subject of a number of quantum chemistry studies indicating that the orbital interaction accounts for about 40% and the electrostatic attraction about 60% of all attractive forces.[33] Our adopted values are taken from *ab initio* calculations considering a B-DNA fragment.[32] Depending on the DNA sequence composition, its length, and the effective temperature, the value of the hopping integral between stacked bases can vary over a relatively broad interval, ranging from $t_0=0.01$ to 0.4 eV.[13,34–39] Our adopted value is based on (i) quantum chemistry calculations yielding $t_0=0.14-0.22$ eV for poly(dG)-poly(dC) and poly(dA)-poly(dT) duplexes in B-DNA geometry,[40] (ii) first-principles calculations for a four-base-pair G-C stacking arranged in B-DNA configuration ($t_0=0.115$ eV),[41] and (iii) previous works where some experimental *I-V* curves for polyG-polyC chains were correctly reproduced by using $t_0=0.17$ eV.[42]

The reliability of our adopted parameters to model the transport properties of DNA can be appreciated by comparing with previous results obtained from more sophisticated first-principles calculations. To this end, we have evaluated the bandwidth of the HOMO and LUMO bands making use of the data tabulated in Table I in the analytical expressions reported in Ref. 16, obtaining $W_{\mathrm{HOMO}}=367$ meV and $W_{\mathrm{LUMO}}=931$ meV. Both bands are separated by a gap of width $\Delta=6.312$ eV. The obtained bandwidths compare reasonably well with the values reported for short (5–12 BPs) polyG-polyC and polyA-polyT chains from first-principles band structure calculations (HOMO bandwidths $\simeq 50-400$ meV; LUMO bandwidths $\simeq 100-300$ meV).[13,34,36,43,44] Assuming, as is usual, that each BP contributes one free charge carrier,[45] the HOMO-LUMO gap width $\Delta=6.79$ eV was obtained. This figure occupies an intermediate position between numerically obtained values for polyG-polyC chains (7.4–7.8 eV),[46] and photoemission spectroscopy measurements (4.5–5.0 eV) performed in polyG-polyC and polyA-polyT chains.[47]

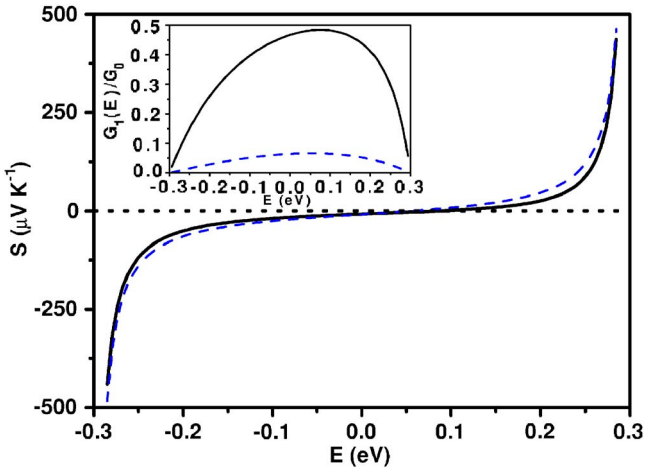

FIG. 2. (Color online) Room temperature dependence of the Seebeck coefficient as a function of the Fermi level energy for a G-C (solid curve) and A-T (dashed curve) Watson-Crick BP. Inset: The Landauer conductance as a function of the Fermi level energy for the same BPs.

In order to illustrate the different energy scales considered in the DNA energetics, in Table I we hierarchically arrange the different parameters included in our tight-binding model, ranging from high energy values related to the sugar-phosphate (12.3 eV) and nucleobase (7.7–9.1 eV) on-site energies, to intermediate energy values related to the base-sugar interaction (1.5 eV) and the complementary base coupling (0.3–0.9 eV), and ending up with the aromatic base stacking low energies (0.15 eV). Finally, in order to reasonably satisfy the condition $\tau=t_M=t_0$, we shall assume a contact geometry corresponding to a DNA chain connected to guanine wires at both sides. In this way, the spectral window is given by the energy interval $[-0.3,0.3]$ eV, where the origin of energies is set at the guanine contact level (i.e., $\varepsilon_M=\varepsilon_G\equiv 0$). Note that the resulting contact bandwidth ($4t_M=0.6$ eV) compares well with the HOMO bandwidths reported for periodic guanosine stacked ribbons from first-principle studies.[48] Although the possible use of organic contacts is just a tentative option, it is clear that in the case of guanine wires the alignment between the contact Fermi level and the DNA HOMO band is properly enhanced. If we consider metallic contacts the potential barrier between the electrode and the DNA molecule is set by the energy difference between the metal Fermi level and the HOMO state of guanine, and typically lies within the range 2.4 eV (platinum leads) and 3.5 eV (gold leads),[12] so that we should properly widen our considered spectral window.

B. Transport curves

In Fig. 2 we plot the thermopower and electrical conductance curves as a function of the Fermi energy obtained from Eqs. (9) and (13) for both G-C and A-T complementary pairs ($N=1$). The $S(E)$ curves exhibit typically metallic values

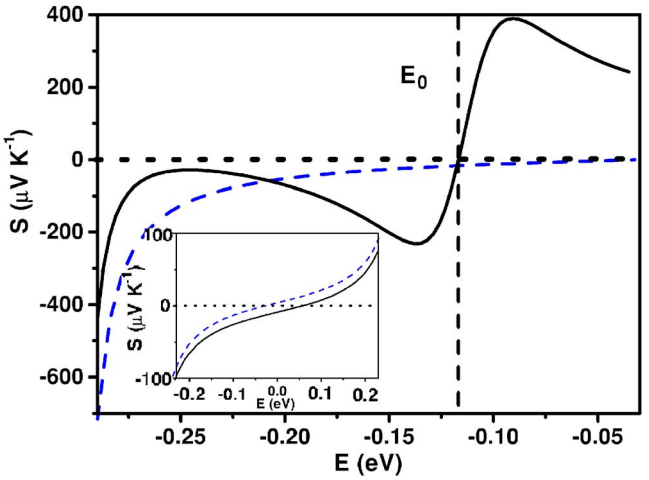

FIG. 3. (Color online) Seebeck coefficient as a function of the Fermi level energy for a polyG-polyC (solid curve) and a polyApolyT (dashed curve) oligomer with $N=5$ BPs. The vertical dashed line separates the energy regions exhibiting n-type and p-type thermopower, respectively. Inset: The Seebeck coefficient as a function of the Fermi level energy for an A-T Watson-Crick BP (solid line) is compared to that correspoding to a polyA-polyT oligomer with $N=5$ (dashed line).

$(1-10\ \mu\ \mathrm{V\ K^{-1}})$ over a broad energy interval around the guanine energy level and then suddenly grow (in absolute value) as E_F approaches the band edges [due to the $B(E_F)$ contribution]. As we can see, the thermoelectric response is very similar for both kinds of Watson-Crick pairs, though the Seebeck coefficient is somewhat larger for the A-T one, due to its smaller conductance value (shown in the inset). In this case $(U_0=1)$ the transmission coefficient reduces to $T_1=(1+C)^{-1}$ and the corresponding conductance curves attain the maximum $G_1 \simeq 3.8\times 10^{-5}$ $(G_1=5.1827\times 10^{-6})\ \Omega^{-1}$ at the resonance energy $E_1^*=8.638\times 10^{-2}$ $(E_1^*=5.501\times 10^{-2})$ eV for G-C (A-T) BPs, respectively. These conductance values are remarkably large (in particular, the G-C BP value is about one order of magnitude larger than the values usually reported for organic molecular junctions[49]) accounting for the small values of the Seebeck coefficient in the energy interval $-0.2 \lesssim E \lesssim 0.2$, as prescribed by the ΔG factor in Eq. (7).

As the number of BPs composing the DNA chain is progressively increased, several topological features (i.e., maxima, minima, and crossing points) appear in the thermopower curves of the polyG-polyC chains, as it is illustrated in Figs. 3 and 6 for the case $N=5$. As we see, the Seebeck coefficient is characterized by the presence of two peaks around a crossing point located at the energy $E_0=-0.116$ eV. The thermopower values attained at the peaks are significantly high, and compare well with the values reported for benchmark thermoelectric materials. Nevertheless, as the Fermi level shifts away from the resonance energy, the Seebeck coefficient significantly decreases, clearly illustrating the fine-tuning capabilities of thermopower measurements. On the contrary, the thermoelectric response of the polyA-polyT chain is rather insensitive to the chain length. This is illustrated in the inset of Fig. 3, where we compare the thermoelectric curves of a single A-T BP and an $N=5$ polyA-polyT oligomer.

This contrasting behavior can be understood by inspecting the conductance curves shown in Fig. 4 for different N values. As we see, the overall topology of the polyA-polyT $G_N(E)$ curves does not substantially change as we progressively increase their length, although the conductance peak ratio G_2/G_5 is significantly reduced by more than five orders of magnitude. This degradation of the charge transport efficiency is related to the fact that both adenine and thymine energy levels are far above the contact Fermi level; meanwhile the guanine level is just aligned to the contact one in the polyG-polyC chain. In that case, a pronounced resonance peak (saturating at the quantum conductance value G_0) appears in the conductance curve, as shown in the inset of Fig. 3. On the other hand, according to Eq. (6) the main features of the polyG-polyC Seebeck coefficient shown in Fig. 2 can

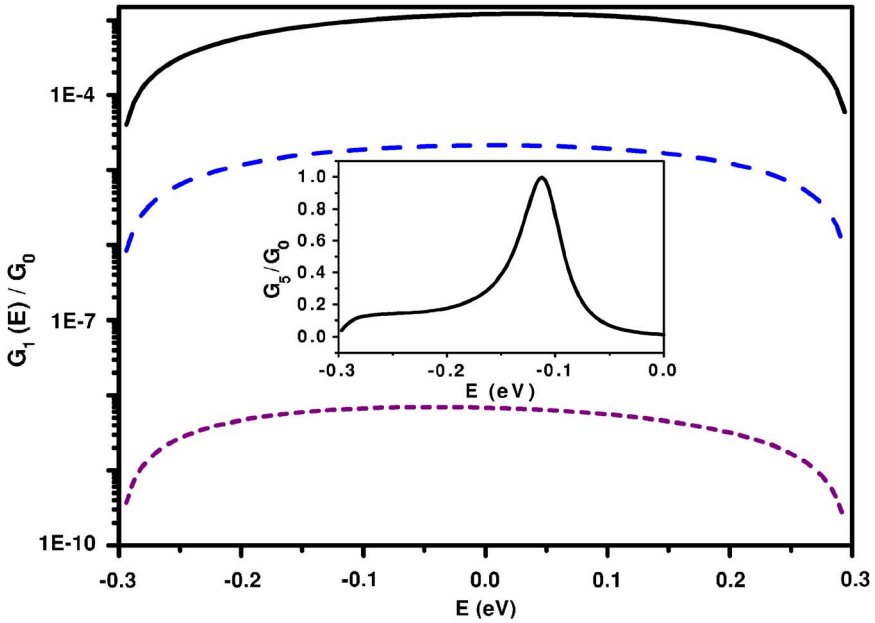

FIG. 4. (Color online) Landauer conductance as a function of the Fermi level energy for polyA-polyT oligomers with $N=2$ (solid curve), 3 (dasehd curve), and 5 (short dashed curve). Inset: Landauer conductance as a function of the Fermi level energy for a polyG-polyC oligomer with $N=5$.

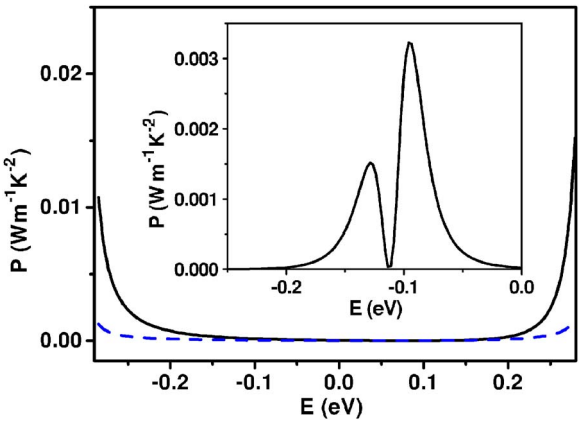

FIG. 5. (Color online) Room temperature thermoelectric power factor as a function of the Fermi level energy for G-C (solid curve) and A-T (dashed curve) Watson-Crick BPs. Inset: Room temperature thermoelectric power factor as a function of the Fermi level energy for a polyG-polyC oligomer with $N=5$.

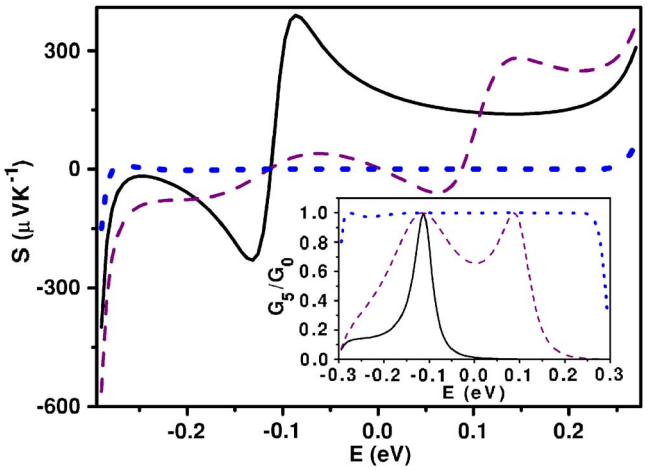

FIG. 6. (Color online) Seebeck coefficient as a function of the Fermi level energy for a polyG-polyC oligomer with $N=5$ BPs and $\gamma=4.5$ (solid curve), 4.0 (dashed curve), and 3.0 eV (dotted curve) with $\tau=t_M=0.15$ eV, and $\varepsilon_M=0$ eV. Inset: Landauer conductance as a function of the Fermi level energy for the same samples shown in the main frame.

be properly accounted for in terms of the conductance curve shown in this inset. In fact, when the Fermi level is located at the left (right) of the conductance peak the slope of the transmission coefficient curve $T_N(E)$ is positive (negative) leading to n-type (p-type) thermopower, respectively. In addition, the steeper the conductance curve the higher the thermopower value close to the resonance energy, as can be readily seen by comparing Figs. 3 and 4. Finally, we note that the crossover energy E_0 defines two different regimes where the polyG-polyC oligomer alternatively exhibits n-type or p-type thermopower. In this regard it is worth mentioning that, when the Fermi level is located above E_0, the Seebeck coefficient of each DNA chain exhibits contrary signs, so that the polyG-polyC chain behaves as a p-type material, while the polyA-polyT chain behaves like an n-type one, in agreement with previous experimental results.[15]

By properly combining the previous results, making use of the typical values $L_N=0.34\times N$ nm for the length and $R=1$ nm for the radius of B-form DNA, we can determine the magnitude of the thermoelectric power factor $P_N=\sigma_N S_N^2=G_N L_N S_N^2/(\pi R^2)$ for the considered samples. In Fig. 5 we plot the power factors of polyG-polyC (solid line) and polyA-polyT (dashed line) chains as a function of the energy for $N=1$ (main frame) and 5 (inset). The overall shape of the power factor is mainly determined by the energy dependence of the Seebeck coefficient. In fact, in the case $N=1$ the power factor takes on relatively small values over a broad range of energies located around the conductance peak, but it significantly increases as the Fermi level approaches the band edges, as was previously discussed. In the case $N=5$, in addition to this general behavior (not shown) we observe that the power factor also attains significantly large values *close* to the resonance energy of the polyG-polyC chain due to the presence of the above mentioned Seebeck coefficient peaks. The values of the power factor maxima attained in this case $[P_5=(1.5-3)\times 10^{-3}\ \mathrm{W\,m^{-1}\,K^{-2}}]$ nicely fit with those reported for benchmark thermoelectric materials $[P=(2.5-3.5)\times 10^{-3}\ \mathrm{W\,m^{-1}\,K^{-2}}]$ at high temperatures.[50] On the contrary, the power factor is completely negligible for polyA-polyT oligonucleotides.

V. ENVIRONMENTAL EFFECTS

Broadly speaking, the electronic DNA energetics includes three different contributions coming from the nucleobase system, the backbone system, and the environment. Environmental effects are related to the presence of counterions and water molecules, interacting with the nucleobases and the backbone by means of hydration, solvation, and charge transfer processes. The energy scale of these interactions (1–5 eV) is about one order of magnitude larger than the hydrogen bonding between Watson-Crick pairs (0.4–0.9 eV) and about two orders of magnitude larger than the base stacking energies (0.01–0.4 eV), as we have previously discussed (see Table I). Up to now, we have neglected the possible influence of environmental effects, keeping a fixed value for the backbone-related on-site energy γ. However, the sensitivity of thermopower to possible backbone effects should be considered in any realistic treatment, for the presence of a number of counterions located along the DNA sugar-phosphate backbone (mainly in the vicinity of negatively charged phosphates) as well as the grooves of the DNA helix (mainly near the nitrogen electronegative atoms of guanine and adenine) is expected.[51] A crude estimation about the influence of the cations on the unperturbed γ value was given in a previous work, where we concluded that γ values within the range $2\leqslant\gamma\leqslant 3$ eV (rather than $\gamma\simeq 4.5$ eV) can be reasonably expected in some realistic situations.[16] In Fig. 6 we compare the Seebeck coefficient as a function of the energy for different γ values for a polyG-polyC chain with $N=5$. By inspecting this plot we realize the remarkable role played by backbone effects on thermopower. In fact, by systematically varying the on-site energy parameter from $\gamma=4.5$ eV (no environmental effects) to $\gamma=3.0$ eV, the thermoelectric response of the DNA chain can be modulated from typically semiconducting values to typically metallic ones. As expected from basic theory [see Eq.

(7)], the degradation of the thermopower is related to a progressive enhancement of the DNA conductance. This result is shown in the inset of Fig. 6, where we plot the systematic variation of the polyG-polyC oligomer conductance as γ is progressively decreased.

On the other hand, as we consider progressively longer chains, the role of thermal and dephasing effects (related to the vibrational degrees of freedom of counterions and hydration shells in DNA) becomes progressively important, eventually leading to a phase coherence break through the system.[52] A possible way to account for dephasing effects within the Landauer approach consists in coupling a dephasing term to every site of the DNA backbone.[53,54] The main effect of such a coupling is then to modify the γ value. In a previous work we explicitly considered the possible influence of a relatively wide fluctuation of such a parameter ($\Delta\gamma = \pm 1$ eV) on the main features of the thermopower curve of single-stranded DNA chains, concluding that the resonance peak in the thermopower curve is quite robust under the influence of local environmental effects.[16] Within the framework of the one-dimensional effective Hamiltonian discussed in this work, we can confidently extrapolate this result to the case of double-stranded DNA chains too, as long as we restrict our discussion to relatively short oligomers.

VI. CONTACT EFFECTS

In order to ascertain the *intrinsic* DNA electrical transport properties one must pay particular attention to the role of contacts. In earlier measurements, DNA contact with metal electrodes was achieved by laying down the molecules directly on the electrodes. In this case, it is rather difficult to prove that the DNA molecule is in direct contact with the electrodes. Even so, the weak physical adhesion between DNA and metal may produce an insulating contact.[12] Recent transport experiments have shown that chemical bonding between DNA and metal electrodes is a prerequisite for achieving reproducible conductivity results.[17,20–24] In a previous work, we considered the role of contact effects in a polyGACT single strand connected to metallic leads at both ends. In general, interference effects between the DNA molecular bands and the electronic structure of the leads at the metal-DNA interface degrades the transmission, as expected. But one also observes that coupling to the leads gives rise to the presence of a set of resonant states in the system, determined by the resonance condition $t_* = \sqrt{t_0 t_M}$, which defines the optimal contact configuration for efficient charge transfer through the entire metal-DNA-metal system.[27]

In the present model for a double-stranded DNA the influence of the metallic contacts on the charge distribution around the phosphate groups closer to the leads can be accounted for by replacing the renormalized on-site energy value given by Eq. (2) by the following one:

$$\alpha_M(E) = a_0 + a_1(E - \gamma_M) + \frac{2t^2}{E - \gamma_M}. \tag{14}$$

Thus, we assume that the contacts have a similar effect on both strands, so that the on-site energies close to the leads take a common value γ_M, which in turn differs from that corresponding to the remaining sites along the backbone, γ. Making use of Eq. (14) in Eq. (3) we obtain

$$\tilde{T}_N(E) = \{1 + W^{-1}[\sqrt{W(T_N^{-1} - 1)} + 4\xi\Omega(HU_{N-2} - U_{N-1})]^2\}^{-1}, \tag{15}$$

where T_N is given by Eq. (4), $H \equiv \lambda \cos k - \xi$, and the auxiliary parameter

$$\xi \equiv \frac{\gamma - \gamma_M}{2t_0}\left(\frac{2t^2}{(E - \gamma)(E - \gamma_M)} - a_1\right) \tag{16}$$

provides a measure of the relative strength of the contact effects (in eV). It is readily checked that in the case $\xi = 0$ Eq. (15) reduces to Eq. (4), as required. In the duplex DNA case, the full transmission condition, corresponding to the optimal choice for the contact parameters is given by the relationship $t_M = t_0 = \tau$, indicating that metal contacts are not the most appropriate choice in order to minimize contact effects, and favor the use of organic crystals to this end. In this sense, the guanine wires recently studied by Di Felice and co-workers, with HOMO bandwidths of about 0.3 eV, appear as very promising candidates.[48]

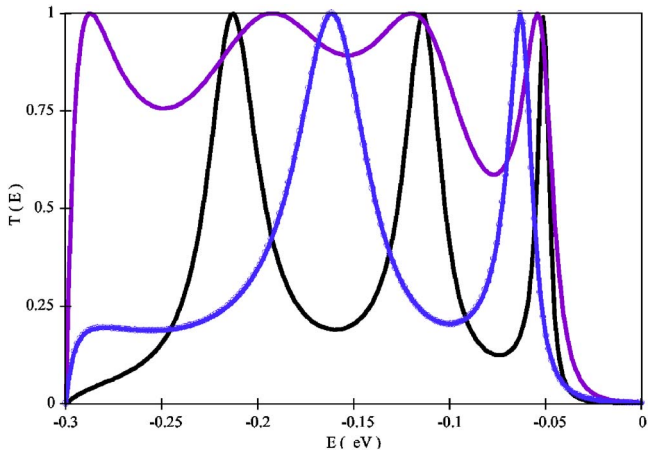

FIG. 7. (Color online) Transmission coefficient as a function of the Fermi level energy, determined from Eq. (15) including contact effects, for a polyG-polyC oligomer with $N=10$ BPs and $\gamma=4.5$ (solid curve), 4.0 (dashed curve), and 3.0 eV (dotted curve) with $\tau = t_M = 0.15$ eV, and $\varepsilon_M = 0$ eV.

In Fig. 7 we show the transmission pattern for a polyG-polyC chain with $N=10$ BPs. As we can see, the main effect of changing the backbone on-site energy value close to the leads is to change the number and relative positions of the full transmission peaks. According to Eq. (6), for a given location of the Fermi level, charge transfer at the end phosphate groups will induce a fluctuation of the Seebeck coefficient value, leading to a beneficial enhancement of the thermoelectric power in most cases.

VII. CONCLUSIONS

From the results reported in previous sections we conclude that the thermoelectric response of short dsDNA chains

strongly depends on (i) the chemical nature of the considered DNA chain and (ii) the relative position between the contact Fermi level and the DNA molecular levels. Thus, while the thermoelectric power of polyA-polyT oligomers is quite insensitive to the number of BPs composing the chain, polyG-polyC oligomers exhibit a strong dependence on the chain length. Accordingly, we can efficiently optimize the power factor of polyG-polyC chains by properly shifting the Fermi level position close to the resonance energy, which plays the role of a tuning parameter. On the other hand, depending on the E_F position, *n*-type and *p*-type thermoelectric responses can be simultaneously obtained for polyA-polyT and polyG-polyC DNA chains, respectively. This is a very convenient feature in order to design DNA-based thermoelectric devices, where both oligomers would play the role that semiconducting materials legs usually play in standard Peltier cells. To this end, the relatively low value of the polyA-polyT chain Seebeck coefficient could be significantly improved by connecting it to adenine wires, rather than guanine ones, in order to get a proper alignment between the contacts Fermi level and the DNA molecular levels.

The thermoelectric quality of a material is expressed in terms of the dimensionless figure of merit $ZT=S^2\sigma T/\kappa = PT/\kappa$, where κ is the thermal conductivity. Therefore, the potential of DNA oligomers as thermoelectric materials will ultimately depend on their thermal transport properties which, to the best of my knowledge, have not yet been fully analyzed. Nevertheless, we can make a rough estimation of ZT by assuming that the thermal transport properties recently reported for a series of simple organic semiconductors (e.g., pentacene) are representative of more complex biomolecules as well. In particular, it seems reasonable to expect that the thermal conduction is dominated by phonon transport in these organic compounds, leading to small thermal conductivities in general. In fact, room temperature thermal conductivity values in the range $\kappa=0.25-0.50$ W m^{-1} K^{-1} were measured for different organic films.[55] It is well known that the thermal conductivity of low dimensional systems is usually lower than the bulk, accounting for the higher thermoelectric performance reported for multilayers and nanowires.[56] Accordingly, bulk values provide an upper limit to the expected thermal conductivity. A suitable estimation of thermal conductivity for ideal coupling between a ballistic thermal conductor and the reservoirs relies on the quantum of thermal conductance $g_0=\pi^2k_B^2T/(3h)=9.46\times10^{-13}T$ W K^{-1}, which represents the maximum possible value of energy transported per phonon mode.[57] In the regime of low temperatures four main modes, arising from dilatational, torsional, and flexural degrees of freedom, are expected for a quantum wire.[58] Therefore, the thermal conductivity of a DNA oligomer of length $L_N=0.34N$ nm will be given by $\kappa_N\simeq 4g_0L_N/(\pi R^2)=0.02$ W m^{-1} K^{-1} (at $T=10$ K) and $\kappa_N\simeq 0.6$ W m^{-1} K^{-1} (at room temperature) in optimal conditions. By taking the value $\kappa\simeq 0.1$ W m^{-1} K^{-1} as a suitable reference value, along with the power factor values previously obtained, we get $ZT\simeq 4.5-9.0$ for polyG-polyC chains with five BPs at room temperature (well above the usual highest $ZT\simeq 1$ for conventional bulk materials). These remarkably high figure of merit values (comparable to those exhibited by the best thermoelectric materials[59,60]) must be properly balanced with the significant role played by unavoidable environmental effects, stemming from the presence of a cation and/or water molecule atmosphere around the DNA chain, on the actual thermoelectric efficiency of DNA-based nanocells. The inclusion of phonon degrees of freedom, following the approaches introduced in some recent works,[61,62] would be then pertinent in order to obtain more accurate estimations on the feasibility of this proposal. In particular, the role of polarons (whose formation is a very common process for organic polymers with a flexible backbone such as DNA) in the electrical transport efficiency will deserve a closer scrutiny.[15,63–65,67] Broadly speaking, the on-site interaction of the charge carrier with phonon modes tends to localize it, leading to charge transfer rates within the range $\tau=5-75$ ps, as reported by experiments.[66] These values are much longer than the charge transfer rates related to coherent tunneling (the dominant process assumed in our approach), which are given by $\tau\simeq t_0/h\simeq 0.03$ ps. Accordingly, one reasonably expects that the presence of polarons gives rise to a degradation of the charge transfer efficiency, as compared to that corresponding to coherent transport conditions. From basic principles one knows that a decrease in the charge transfer efficiency is generally accompanied by an enhancement of the Seebeck coefficient in most samples. On this basis, one could then expect that the inclusion of polaronic effects would lead to further improvement in the thermoelectric properties of DNA chains.

In summary, our theoretical prospective study on the thermoelectric properties of synthetic DNA oligonucleotides clearly indicates that these materials are suitable candidates to be considered in the design of highly performing, nanoscale-sized thermoelectric cells. Experimental work aimed to test the actual capabilities of DNA-based thermoelectric devices under different environmental conditions as well as to accurately determine the thermal transport properties of synthetic DNA samples would be very appealing.

ACKNOWLEDGMENTS

I warmly thank E. Artacho, G. Cuniberti, R. Di Felice, R. Gutierrez, D. Porath, S. Roche, E. B. Starikov, and M. Zwolak for sharing useful information. I acknowledge M. V. Hernández for a critical reading of the manuscript. This work has been supported by the Universidad Complutense de Madrid through Project No. PR27/05-14014-BSCH.

[1] J. C. Poler, R. M. Zimmermann, and E. C. Cox, Langmuir **11**, 2689 (1995).
[2] M. Paulsson and S. Datta, Phys. Rev. B **67**, 241403(R) (2003).
[3] X. Gao, K. Uehara, D. D. Klug, J. S. Tse, and T. M. Tritt, Phys. Rev. B **72**, 125202 (2005).
[4] K. Esfarjani, M. Zebarjadi, and Y. Kawazoe, Phys. Rev. B **73**, 085406 (2006).
[5] S. Roche and E. Maciá, Mod. Phys. Lett. B **18**, 847 (2004).
[6] E. Maciá, Nanotechnology **16**, S254 (2005).
[7] E. Maciá, Rev. Adv. Mater. Sci. **10**, 166 (2005).
[8] X. Zheng, W. Zheng, Y. Wei, Z. Zeng, and J. Wang, J. Chem. Phys. **121**, 8537 (2004).
[9] J. Lagerqvist, M. Zwolak, and M. Di Ventra, Nano Lett. **6**, 779 (2006).
[10] M. Zwolak, and M. Di Ventra, Nano Lett. **5**, 421 (2005).
[11] E. Maciá, Rep. Prog. Phys. **69**, 397 (2006).
[12] R. G. Endres, D. L. Cox, and R. R. P. Singh, Rev. Mod. Phys. **76**, 195 (2004).
[13] E. Artacho, M. Machado, D. Sánchez-Portal, P. Ordejón, and J. M. Soler, Mol. Phys. **101**, 1587 (2003).
[14] E. B. Starikov, Philos. Mag. **85**, 3435 (2005).
[15] K. H. Yoo, D. H. Ha, J. O. Lee, J. W. Park, J. Kim, J. J. Kim, H. Y. Lee, T. Kawai, and H. Y. Choi, Phys. Rev. Lett. **87**, 198102 (2001).
[16] E. Maciá, and S. Roche, Nanotechnology **17**, 3002 (2006).
[17] D. Porath, A. Bezryadin, S. de Vries, and C. Dekker, Nature (London) **403**, 635 (2000); H. Cohen, C. Nogues, R. Naaman, and D. Porath, Proc. Natl. Acad. Sci. U.S.A. **102**, 11589 (2005).
[18] J. S. Hwang, K. J. Kong, D. Ahn, G. S. Lee, D. J. Ahn, and S. W. Hwang, Appl. Phys. Lett. **81**, 1134 (2002).
[19] A. J. Storm, J. van Noort, S. de Vries, and C. Dekker, Appl. Phys. Lett. **79**, 3881 (2001).
[20] Y. Zhang, R. H. Austin, J. Kraeft, E. C. Cox, and N. P. Ong, Phys. Rev. Lett. **89**, 198102 (2002).
[21] B. Hartzell, B. Melord, D. Asare, H. Chen, J. J. Heremans, and V. Sughomonian, Appl. Phys. Lett. **82**, 4800 (2003).
[22] J. Hihath, B. Xu, P. M. Zhang, and N. J. Tao, Proc. Natl. Acad. Sci. U.S.A. **102**, 16979 (2005); B. Xu, P. M. Zhang, X. L. Li, and N. J. Tao, Nano Lett. **4**, 1105 (2004).
[23] T. Heim, D. Deresmes, and D. Vuillaume, J. Appl. Phys. **96**, 2927 (2004).
[24] M. S. Xu, R. G. Endres, S. Tsukamoto, M. Kitamura, S. Ishida, and Y. Arakawa, Small **1**, 168 (2005).
[25] E. G. Emberly and G. Kirczenow, Phys. Rev. B **58**, 10911 (1998); J. Phys.: Condens. Matter **11**, 6911 (1999).
[26] T. Kostyrko, J. Phys.: Condens. Matter **14**, 4393 (2002).
[27] E. Maciá, F. Triozon, and S. Roche, Phys. Rev. B **71**, 113106 (2005).
[28] K. Iguchi, Int. J. Mod. Phys. B **18**, 1845 (2004).
[29] M. Büttiker, Y. Imry, R. Landauer, and S. Pinhas, Phys. Rev. B **31**, 6207 (1985).
[30] Essentially describing a diffusive behavior of the charge carriers. Possible electron-phonon interactions, giving rise to phonon-drag effects at low temperatures, are not included in our treatment. According to photoinduced infrared spectroscopy measurements a relatively low hole-vibrational coupling constant ($\lambda \approx 0.2$) is expected for biological dsDNA samples, as was reported by A. Omerzu, M. Licer, T. Mertelj, V. V. Kabanov, and D. Mihailovic, Phys. Rev. Lett. **93**, 218101 (2004).
[31] The role of contact effects in the charge transfer efficiency through DNA molecules was studied in detail in Ref. 27.
[32] Y. J. Yan and H. Zhang, J. Theor. Comput. Chem. **1**, 225 (2002).
[33] C. Fonseca Guerra, F. M. Bickelhaupt, and E. J. Baerends, Cryst. Growth Des. **2**, 239 (2002). Taking the value 25 kcal/mol for the G-C energy coupling, one gets $t_{GC} \simeq 0.4$ eV for the orbital overlapping contribution.
[34] P. J. de Pablo, F. Moreno-Herrero, J. Colchero, J. Gomez Herrero, P. Herrero, A. M. Baro, P. Ordejón, J. M. Soler, and E. Artacho, Phys. Rev. Lett. **85**, 4992 (2000).
[35] R. Di Felice, A. Calzolari, E. Molinari, and A. Garbesi, Phys. Rev. B **65**, 045104 (2002).
[36] H. Wang, J. P. Lewis, and O. F. Sankey, Phys. Rev. Lett. **93**, 016401 (2004).
[37] Y. A. Berlin, M. L. Burin, and M. A. Ratner, Superlattices Microstruct. **28**, 241 (2000).
[38] H. Sugiyama and I. Saito, J. Am. Chem. Soc. **118**, 7063 (1996).
[39] A. A. Voityuk, J. Jortner, M. Bixon, and N. Rösch, J. Chem. Phys. **114**, 5614 (2001).
[40] E. B. Starikov, Philos. Mag. Lett. **83**, 699 (2003).
[41] H. Mehrez and M. P. Anantram, Phys. Rev. B **71**, 115405 (2005).
[42] G. Cuniberti, L. Craco, D. Porath, and C. Dekker, Phys. Rev. B **65**, 241314(R) (2002).
[43] J. P. Lewis, P. Ordejón, and O. F. Sankey, Phys. Rev. B **55**, 6880 (1997).
[44] Ch. Adessi and M. P. Anantram, Appl. Phys. Lett. **82**, 2353 (2003); Ch. Adessi, S. Walch, and M. P. Anantram, Phys. Rev. B **67**, 081405(R) (2003).
[45] The electrical conductance of both periodic and aperiodic DNA molecules with varied density of charge carriers has been recently discussed by X. Gao, X. Fu, L. M. Mei, and S. J. Xie, J. Chem. Phys. **124**, 234702 (2006).
[46] D. M. York, T. S. Lee, and W. Yang, Phys. Rev. Lett. **80**, 5011 (1998).
[47] H. S. Kato, M. Furukawa, M. Kawai, M. Taniguchi, T. Kawai, T. Hatsui, and N. Kosugi, Phys. Rev. Lett. **93**, 086403 (2004); H. Wadat, K. Okazaki, Y. Niimi, A. Fujimori, H. Tabata, J. Pikus, and J. P. Lewis, Appl. Phys. Lett. **86**, 023901 (2005).
[48] R. Di Felice, A. Calzolari, and H. Zhang, Nanotechnology **15**, 1256 (2004); A. Calzolari, R. Di Felice, E. Molinari, and A. Garbesi, J. Phys. Chem. B **108**, 2509 (2004); A. Calzolari, R. Di Felice, and E. Molinari, Appl. Phys. Lett. **80**, 3331 (2002); A. Calzolari, R. Di Felice, E. Molinari, and A. Garbesi, Physica E (Amsterdam) **13**, 1236 (2002).
[49] C. Kergueris, J. P. Bourgoin, S. Palacin, D. Esteve, C. Urbina, M. Magoga, and C. Joachim, Phys. Rev. B **59**, 12505 (1999).
[50] S. Yamaguchi, Y. Nagawa, N. Kaiwa, and A. Yamamoto, Appl. Phys. Lett. **86**, 153504 (2005).
[51] R. N. Barnett, C. L. Cleveland, A. Joy, U. Landman, and G. B. Schuster, Science **294**, 567 (2001).
[52] D. Porath, G. Cuniberti, and R. Di Felice, in *Long-Range Charge Transfer in DNA II*, edited by G. Schuster, Topics in Current Chemistry Vol. 237 (Springer-Verlag, Heidelberg, 2004), p. 183.
[53] X. Q. Li and Y. J. Yan, Appl. Phys. Lett. **79**, 2190 (2001).
[54] R. Gutiérrez, S. Mandal, and G. Cuniberti, Phys. Rev. B **71**, 235116 (2005).
[55] N. Kim, B. Domercq, S. Yoo, A. Christensen, B. Kippelen, and S. Grahm, Appl. Phys. Lett. **87**, 241908 (2005).
[56] G. S. Nolas, J. Sharp, and H. J. Goldsmid, *Thermoelectrics: Basic Principles and New Materials Developments*, Springer Series in Materials Science Vol. 45 (Springer, Berlin, 2001), p. 235.
[57] K. Schwab, E. A. Henriksen, J. M. Worlock, and M. L. Roukes,

Nature (London) **404**, 974 (2000).
[58] N. Nishiguchi, Phys. Rev. B **52**, 5279 (1995); N. Nishiguchi, Y. Ando, and M. N. Wybourne, J. Phys.: Condens. Matter **9**, 5751 (1997).
[59] T. C. Harman, P. J. Taylor, M. P. Walsh, and B. E. LaForge, Science **297**, 2229 (2002).
[60] *Recent Trends in Thermoelectric Materials Research III*, edited by T. M. Tritt, Semiconductors and Semimetals Vol. 71 (Academic Press, San Diego, CA, 2001).
[61] D. Segal, Phys. Rev. B **72**, 165426 (2005).
[62] J. Koch, F. von Oppen, Y. Oreg, and E. Sela, Phys. Rev. B **70**, 195107 (2004).
[63] E. M. Conwell and S. V. Rakhmanova, Proc. Natl. Acad. Sci. U.S.A. **97**, 4556 (2000).
[64] W. Zhang, A. O. Govorov, and S. E. Ulloa, Phys. Rev. B **66**, 060303(R) (2002).
[65] S. S. Alexandre, E. Artacho, J. M. Soler, and H. Chacham, Phys. Rev. Lett. **91**, 108105 (2003).
[66] C. Wan, T. Fiebig, S. O. Kelley, C. R. Treadway, J. K. Barton, and A. H. Zewail, Proc. Natl. Acad. Sci. U.S.A. **96**, 6014 (1999).
[67] H. Yamada, E. B. Starikov, D. Hennig, and J. F. R. Archilla, Eur. Phys. J. E **17**, 149 (2005).